263 (1968).

[2]J. W. Stewart, J. Phys. Chem. Solids 1, 146 (1956).

[3]J. deBoer and B. S. Blaisse, Physica 14, 149 (1948).

[4]K. F. Herzfeld and M. Goeppert-Mayer, Phys. Rev. 46, 995 (1934).

[5]J. deBoer, in Progress in Low Temperature Physics II (North-Holland, Amsterdam, 1957).

[6]F. W. DeWette and B. R. A. Nijboer, Phys. Letters 18, 19 (1965).

[7]N. Bernades, Phys. Rev. 112, 1534 (1958).

[8]N. Bernades and H. Primakoff, Phys. Rev. 119, 968 (1960).

[9]R. P. Hurst and J. M. H. Levelt, J. Chem. Phys. 34, 54 (1961).

[10]J. M. H. Levelt and R. P. Hurst, J. Chem. Phys. 32, 96 (1960).

[11]E. M. Saunders, Phys. Rev. 126, 1724 (1962).

[12]L. H. Nosanow, Phys. Rev. Letters 13, 270 (1964).

[13]W. J. Mullin, Phys. Rev. 134, A1249 (1964).

[14]J. P. Hansen and D. Levesque, Phys. Rev. 165, 293 (1968).

[15]K. A. Brueckner and T. Frohberg, Progr. Theoret. Phys. (Kyoto), Extra Suppl., 383 (1965).

[16]W. E. Massey and C. W. Woo, Phys. Rev. 169, 241 (1968).

[17]L. Pauling, Phys. Rev. 36, 430 (1930).

[18]A. Brooks Harris, Phys. Rev. B 1, 1881 (1970).

[19]D. J. Thouless, The Quantum Mechanics of Many Body Systems (Academic, New York, 1961).

[20]L. H. Nosanow and W. J. Mullin, Phys. Rev. Letters 14, 133 (1965).

[21]J. O. Hirschfelder, C. F. Curtiss, and R. B. Bird, Molecular Theory of Gases and Liquids (Wiley, New York, 1954), pp. 1083–1092.

[22]N. G. Van Kampen, Physica 27, 783 (1961).

[23]J. H. Hetherington, W. J. Mullin, and L. H. Nosanow, Phys. Rev. 154, 175 (1967).

[24]Hard-core models have been used for high-density quantum gas calculations [see R. K. Cole, Jr., Phys. Rev. 155, 114 (1967)].

[25]F. Iwamoto and M. Yamada, Progr. Theoret. Phys. (Kyoto) 17, 543 (1957).

[26]A. M. Michels, W. deGraaf, and C. A. ten Seldam, Physica 26, 393 (1960).

[27]I. B. Srivastava and A. K. Barua, Indian J. Phys. 35, 320 (1961).

[28]K. Tomita, Proc. Phys. Soc. (London) A68, 214 (1955)

[29]T. Nakamura, Progr. Theoret. Phys. (Kyoto) 14, 135 (1955).

[30]R. L. Mills and A. F. Schuch, Phys. Rev. Letters 15, 722 (1965).

Equation of State for Solid Hydrogen[*]

Thomas Alexander Bruce

Laboratory of Atomic and Solid State Physics, Cornell University, Ithaca, New York 14850

(Received 24 May 1971)

An equation of state for solid hydrogen is obtained from variational calculations for pressures up to 112 kbar. The Lennard-Jones potential is assumed and a brief investigation of the Buckingham exp-6 potential is also made. It is suggested that for high densities, quantum crystals may become harmonic and that Monte Carlo variational calculations for these high-density regions may not be necessary.

I. INTRODUCTION

During the last several years there has been a growing interest in the properties of solid hydrogen.[1,2]

The properties of the predicted high-density metallic phase have been discussed in detail by Ashcroft.[2] To predict the existence of this phase requires an accurate equation of state for both the molecular and metallic phases. This paper will be concerned with the first of these phases; we attempt a first refinement of the equation of state for the molecular phase which should ultimately enable a more precise prediction of the transition pressure. We must at once point out that there is considerable uncertainty in the intermolecular potential and thus any highly refined calculations are not very valuable at this time. Indeed the

only useful purpose such calculations can serve at the present time is to remove some of the uncertainty in the potential. It is for this reason that we have limited our Monte Carlo calculations to fairly small numbers of particles and intermediate-length runs.

Krumhansl and Wu[3] have used the cluster-expansion method to do a variational calculation of the equation of state of molecular hydrogen in the 0–20-kbar range. However, Monte Carlo calculations are more reliable because the trial wave functions that may be used are not as limited as those which can be used in the cluster method, and the convergence of the cluster expansion is sometimes uncertain.

In the present study, a trial wave function is chosen, and the integrals necessary to calculate the ground-state energy are evaluated by a Monte

Carlo integration scheme. The method follows closely the earlier calculations for solid helium by Hansen and Levesque[4] and solid neon by Hansen.[5]

II. FORMALISM

A. Hamiltonian

The major part of our work has been done using the 6-12 Lennard-Jones potential:

$$V(r) = 4\epsilon \left[(\sigma/r)^{12} - (\sigma/r)^6 \right] \quad . \tag{2.1}$$

We have used a reduced system of units so that in this paper, unless otherwise stated, all distances will be expressed in units of σ, and all energies in degrees Kelvin. The numerical values for ϵ and σ are determined from the experimental second virial coefficients,[6] and in this work we have taken $\epsilon = 36.7$ °K and $\sigma = 2.958$ Å. The Hamiltonian for N molecules of mass m is then

$$H = -\frac{h^2}{2m} \sum_{i=1}^{N} \nabla_i^2 + \sum_{i<j} V(r_{ij}) \quad , \tag{2.2}$$

where

$$r_{ij} = |\vec{r}_i - \vec{r}_j| \quad .$$

The Lennard-Jones potential is particularly convenient because the two terms of the potential scale with the density. We have made extensive use of this property throughout our work.

We have also made a brief investigation of the modified Buckingham "exp-6" potential developed by Srivastava and Barua[7] and used by Krumhansl and Wu:

$$V(r) = \begin{cases} \dfrac{\epsilon}{1 - 6/\alpha} \left\{ \dfrac{6}{\alpha} \exp\left[\alpha \left(1 - \dfrac{r}{rm} \right) \right] \right. \\ \qquad \left. - \left(\dfrac{rm}{r} \right)^6 \right\}, \quad r > r_{\max} \\ \infty, \qquad\qquad\qquad r < r_{\max} \end{cases} \tag{2.3}$$

where ϵ is the depth of the potential, r_m is the position of the minimum, α is a parameter which gives a measure of the steepness of the repulsive part of the potential, and $r_{\max}$ is the value of r for which $V(r)$ has a maximum. The parameters for hydrogen have been determined by Srivastava et al.[7] and are

$$\alpha = 14.0, \qquad r_m = 3.339 \text{ Å},$$

$$\epsilon = 38.02 \text{ °K}, \qquad r_{\max} = 0.7864 \text{ Å}.$$

B. Trial Wave Function

The trial wave function is

$$\psi = \prod_{i<j} f(r_{ij}) \prod_i \Phi(r_i) \quad ,$$

where the $\Phi(\vec{r}_i)$ are one-particle wave functions centered on the lattice sites and $f(r_{ij})$ is a spherically symmetric two-body correlation function.

The wave function is neither symmetric nor anti-symmetric, but is convenient since, for a solid, the particles are localized on lattice sites and are thus distinguishable, for all practical considerations.

In Monte Carlo calculations we are limited by machine space and computation time to a small number of particles. (Most of our calculations have been done with an fcc lattice and 256 particles.) It is desired that the calculations represent the bulk properties of the solid so it is important that the local environment of each particle be similar to that of a particle in a bulk sample. We do this by making the wave function periodic on the boundaries of the cube. Each particle in the cube (of side S) has an image particle at a distance of $\pm S$ in the x, y, and z directions, and the distance r_{ij} between particle i and particle j is taken to be the distance between particle i and the nearest image of particle j.

For the single-particle localization wave function Φ we have chosen a spherically symmetric Gaussian centered on the lattice sites:

$$\Phi(\vec{r}_i) = e^{-(1/2)A|\vec{r}_i - \vec{R}_i|^2} \quad . \tag{2.4}$$

Here the $\vec{R}_i (i = 1 \text{ to } N)$ are the coordinates of the lattice sites and A controls the width of the Gaussian.

For the two-particle correlation function we chose

$$f(r) = e^{-(1/2)u(r)} \quad , \tag{2.5}$$

where

$$u(r) = (B/r)^n \quad . \tag{2.6}$$

The parameter B determines the radius at which the pair function "cuts off" and n determines the sharpness of the cutoff. Previous results[4,8] have shown that for variational calculations, the results are only slightly dependent on n for n between 4 and 5. In this work, n is taken to be 5 and A and B are our variational parameters.

So finally, our trial wave function is

$$\psi = \exp\left[-\tfrac{1}{2} A \sum_i |\vec{r}_i - \vec{R}_i|^2 - \tfrac{1}{2} \sum_{i<j} (B/r_{ij})^5 \right] \quad . \tag{2.7}$$

This is the same wave function as used by Hansen and Levesque[4] in their calculations for solid helium and by Hansen[5] in his calculations for solid neon.

There are two basic approximations in our calculations: (i) The intermolecular potential (in our case the Lennard-Jones or Buckingham exp-6 potential) is spherical and independent of the orientation of the H_2 molecules, and (ii) the correlation function $f(r)$ is a two-body correlation function and is also spherically symmetric. These approximations require some justification. The spherical symmetry assumed in both of these approximations

may at first seem rather absurd. A first guess of the "shape" of the H_2 molecule would normally be that it looks something like a dumbbell. However, calculations by Kolos and Roothaan[9] have shown that the deviation from sphericity for the H_2 molecule is only ~ 8%. (They have calculated $\langle r^2 \rangle = 2.5430a_0^2$ and $\langle 3z^2 - r^2 \rangle = 0.5157a_0^2$, i.e., $\langle r^2 \rangle^{1/2} \approx 0.84$ Å and $\langle 3z^2 \rangle^{1/2} \approx 0.92$ Å. For a spherical molecule, $\langle r^2 \rangle = \langle x^2 + y^2 + z^2 \rangle = \langle 3z^2 \rangle$.) It is this result which suggests that a spherical approximation both to the potential and correlation function may be a good semiapproximation.

We have used a correlation function containing only two-body correlations since very little is known at present about three- or more body correlations. However, contributions from three- or more body correlation are thought to be quite small, and certainly appear to be so in the liquid and solid phases of helium four.[4,8]

C. Expressions for Expectation Values

The energy expectation value is obtained using (2.2) and (2.7):

$$\langle \psi | H | \psi \rangle / \langle \psi | \psi \rangle = \langle T \rangle + \langle V \rangle \quad , \tag{2.8}$$

where $\langle T \rangle$ and $\langle V \rangle$ are, respectively, the mean kinetic and potential energies;

$$\langle T \rangle = N \frac{3h^2}{4m} A + \frac{h^2}{4m} \sum_{i<j} \frac{\int \psi^2 \nabla_{ij}^2 u(r_{ij}) d^3\vec{r}_1 \cdots d^3\vec{r}_N}{\int \psi^2 d^3\vec{r}_1 \cdots d^3\vec{r}_N} , \tag{2.9}$$

$$\langle V \rangle = \sum_{i<j} \frac{\int \psi^2 V(r_{ij}) d^3\vec{r}_1 \cdots d^3\vec{r}_N}{\int \psi^2 d^3\vec{r}_1 \cdots d^3\vec{r}_N} \quad . \tag{2.10}$$

As noted in Ref. 4, "Our quantum-mechanical problem for the evaluation of the expectation value of the energy in the state described by ψ is formally equivalent to the classical calculation of the mean value of the Hamiltonian ... in the canonical ensemble for a fictitious system at the arbitrary 'temperature' T. Such classical calculations by the Monte Carlo method have been introduced by Metropolis and co-workers,[10] and by Wood and Parker."[11] The technical details for the calculation are laid out in the Wood and Parker paper.

We obtain the expectation values $\langle T \rangle$ and $\langle V \rangle$ by first calculating $\langle (\sigma/r)^6 \rangle$, $\langle (\sigma/r)^7 \rangle$, and $\langle (\sigma/r)^{12} \rangle$. From (2.9) we have

$$\langle T \rangle = N \frac{h^2}{4m} A + \frac{5h^2 B^5}{m} \sum_{i<j} \frac{\int \psi^2 r^{-7} d^3\vec{r} \cdots d^3\vec{r}_N}{\int \psi^2 d^3\vec{r}_1 \cdots d^3\vec{r}_N} \quad . \tag{2.11}$$

Since we are measuring all distances in units of σ, this becomes

$$\langle T \rangle = N \frac{h^2}{4m} A + \frac{5h^2 B^5}{m\sigma^2} \sum_{i<j} \left\langle \left(\frac{\sigma}{r} \right)^7 \right\rangle \quad . \tag{2.12}$$

From (2.10) we have

$$\langle V \rangle = \sum_{i<j} \frac{\int \psi^2 \{4\epsilon [(\sigma/r)^{12} - (\sigma/r)^6]\} d^3\vec{r}_1 \cdots d^3\vec{r}_N}{\int \psi^2 d^3\vec{r}_1 \cdots d^3\vec{r}_N} \tag{2.13}$$

$$= 4\epsilon \sum_{i<j} \left[\left\langle \left(\frac{\sigma}{r_{ij}} \right)^{12} \right\rangle - \left\langle \left(\frac{\sigma}{r_{ij}} \right)^6 \right\rangle \right] \quad . \tag{2.14}$$

We can obtain the ground-state virial pressure from these same expectation values,

$$P = \rho \left[\tfrac{2}{3} \langle T \rangle + 16\epsilon \langle (\sigma/r)^{12} \rangle - 8\epsilon \langle (\sigma/r)^6 \rangle \right] \quad . \tag{2.15}$$

The pressure can also be obtained from the thermodynamic expression

$$P = - \frac{dE}{dV} = \rho^2 \frac{dE}{d\rho} \quad . \tag{2.16}$$

The equality of the virial and thermodynamic pressure only holds when the exact ground-state wave function is used. We can therefore expect a difference between the pressures calculated using (2.15) and (2.16). This difference will give us a hint of how good an approximation our trial wave function is.

Our calculations are carried out using N particles located inside of a cube of side S. However in calculating the expectation values $\langle (\sigma/r)^6 \rangle$, $\langle (\sigma/r)^7 \rangle$, and $\langle (\sigma/r)^{12} \rangle$, we take into account only those particles which are separated by a distance $r_{ij} \leq \tfrac{1}{2} S$. This in effect changes our correlation function $f(r_{ij})$ to

$$f(r_{ij}) = \begin{cases} e^{-(1/2)u(r)} , & r_{ij} \leq \tfrac{1}{2} S \\ 0 , & r_{ij} > \tfrac{1}{2} S \end{cases} \quad .$$

In order to correct for those particles which lie at a distance greater than $\tfrac{1}{2} S$ from a particle which is being used in calculating an average, but still within the cube (i.e., outside the "Monte Carlo sphere") we add on contributions to $\langle T \rangle$ and $\langle V \rangle$ from the lattice sites in this "corner point" region. To perform this correction we used the same method as Hansen and Levesque.[4] These "corner" corrections amount to about 3% of the total energy.

Now that we have an expression for $\langle H \rangle$ as a function of A and B we proceed as follows. Using the Monte Carlo integration scheme we calculate the ground-state energy $\langle H \rangle$ for a fixed density ρ_0 for several values of A and B. We then find the minimum of $\langle H \rangle$ as a function of A and B for this density. This gives us a value of the ground-state energy E which is an upper bound on the exact ground-state energy. Then using the scaling formula discussed in Sec. III A we can find the ground-state energy for other densities $\rho \neq \rho_0$. We will then have a curve for E vs ρ from which we can obtain the equation-of-state curves, E vs pressure P.

TABLE I. Results of the Monte Carlo runs which were used for the scaling.

ρ	A	B	$\langle (\sigma/r)^6 \rangle$	$\langle (\sigma/r)^7 \rangle$	$\langle (\sigma/r)^{12} \rangle$	$\langle T \rangle$	$\langle V \rangle$	$\langle H \rangle$
0.694	15	1.15	2.142 78	1.740 70	1.031 43	77.7937	−163.146	− 85.3525
	20	1.15	2.106 83	1.698 20	0.960 393	87.0873	−168.297	− 81.2102
	20	1.20	2.059 40	1.641 30	0.849 958	96.1604	−177.547	− 81.3865
	25	1.25	2.027 24	1.603 59	0.788 619	105.067	−181.830	− 76.7623
0.90	30	1.15	3.356 82	2.873 71	2.056 83	139.543	−190.839	− 51.2963
	30	1.20	3.299 91	2.801 79	1.886 12	155.719	−207.544	− 54.8246
	30	1.25	3.256 07	2.746 74	1.761 49	174.869	−219.404	− 44.5345
1.12	33	1.10	5.150 90	4.721 97	4.702 33	170.420	− 65.8510	104.569
	33	1.15	5.074 91	4.619 13	4.361 02	193.305	−104.799	88.5065
	35	1.15	5.059 58	4.599 52	4.315 46	196.842	−109.236	87.6060
	33	1.20	4.495 61	4.513 13	4.036 43	219.631	−140.808	78.8233
	35	1.20	4.988 33	4.502 69	3.997 69	223.351	−145.427	77.9240
	33	1.25	4.943 27	4.443 57	3.829 09	251.267	−163.562	87.7047
	35	1.25	4.934 77	4.431 68	3.791 29	254.864	−167.863	86.9828
	35	1.30	4.886 37	4.367 47	3.140 19	291.384	−187.853	103.531
	35	1.35	3.847 41	4.317 28	3.489 91	334.043	−199.281	134.763
	35	1.40	4.795 29	4.247 99	3.289 11	381.389	−221.108	160.281
	35	1.45	4.765 37	4.208 74	3.186 56	437.452	−231.768	205.684

III. CONFIGURATION SPACE INTEGRAL

Details of Calculation

Using the standard Monte Carlo integration scheme,[4,10-12] it is possible to find a minimum in $\langle H \rangle$ at any density we choose. The information gained from such a search can be used to calculate the energy for other densities by using a scaling formula first developed by McMillan,[8] and later employed by Hansen and Levesque[4] in their calculations for solid He. If $\rho' \neq \rho$ and we define

$$S = (\rho'/\rho)^{1/3}, \quad A' = AS^2, \quad B' = B/S, \quad (3.1)$$

then the scaling formula for the ground-state energy is

$$E(A', B', \rho') = \langle T \rangle_{A,B,\rho} S^2$$

$$+ 4\epsilon [\langle (\sigma/r)^{12} \rangle_{A,B,\rho} S^{12} - \langle (\sigma/r)^6 \rangle_{A,B,\rho} S^6] . \quad (3.2)$$

The virial pressure can be similarly scaled:

$$P(A', B', \rho') = \rho' \{ \tfrac{2}{3} \langle T \rangle_{A,B,\rho} S^2$$

$$+ 4\epsilon [4 \langle (\sigma/r)^{12} \rangle_{A,B,\rho} S^{12} - 2 \langle (\sigma/r)^6 \rangle_{A,B} S^6] \} . \quad (3.3)$$

We started by doing a parameter search in A and B for $\rho = 0.694$ molecules/σ^3, the equilibrium density obtained by Krumhansl and Wu in their cluster-expansion calculations.[3] A search was done for A values ranging from 5 to 30 and B varying from 1.0 to 1.3. A new search was then made at $\rho = 0.9$, and another at $\rho = 1.12$. Scaling was used to cover the entire region between $\rho = 0.694$ and $\rho = 1.12$.

Our initial search at $\rho = 1.12$ provided enough information so that we could still find an energy minimum, after scaling, up to a density of about 1.23 (equivalent to a pressure of about 10.9 kbar). To go to higher densities there were two alternatives; we could either do a new parameter search at a density of about 1.35 and scale back down to cover the region between 1.23 and 1.35 and up to about 1.5, or we could make a few more runs at $\rho = 1.12$ and use these to extend the range in density for which we could find a minimum in the energy. The first of these would not have been satisfactory since by increasing the density we decrease the size of the "Monte Carlo sphere" in which the averaging process is being done. To compensate for this, we must increase the size of the system—in this case we would have had to go to 500 particles. To sample the configuration

TABLE II. After scaling; values of the parameters A and B which give the minimum in $\langle H \rangle$ and their associated expectation values $\langle (\sigma/r)^6 \rangle$, $\langle (\sigma/r)^7 \rangle$, and $\langle (\sigma/r)^{12} \rangle$.

ρ	A	B	$\langle (\sigma/r)^6 \rangle$	$\langle (\sigma/r)^7 \rangle$	$\langle (\sigma/r)^{12} \rangle$
0.676	14.74	1.160	2.033 07	1.637 17	0.928 514
0.77	21.43	1.159	2.535 15	2.091 66	1.288 02
0.87	29.33	1.163	3.136 76	2.655 15	1.796 00
0.97	29.98	1.154	3.863 59	3.376 10	2.645 62
1.07	33.95	1.218	4.552 89	4.047 54	3.330 21
1.17	36.03	1.183	5.443 66	4.985 75	4.760 81
1.27	38.06	1.199	6.345 10	5.942 03	6.268 01
1.37	40.03	1.216	7.311 25	6.988 80	7.030 17
1.47	41.96	1.279	8.260 64	8.012 14	9.760 58
1.57	43.84	1.251	9.422 76	9.342 02	12.700 0
1.67	45.68	1.225	10.661 3	10.789 8	16.258 2
1.77	47.49	1.245	11.902 5	12.243 8	19.876 6
1.87	49.26	1.222	13.284 5	13.919 0	24.763 8

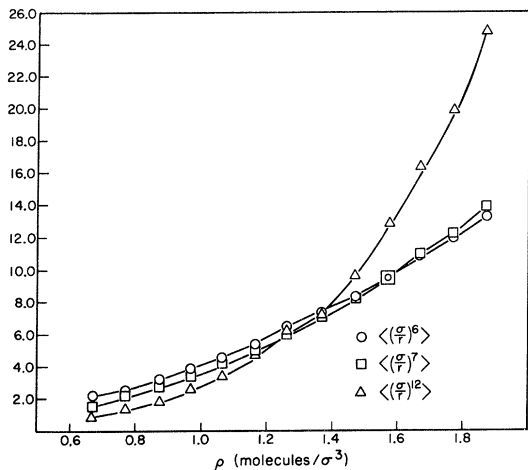FIG. 1. Expectation values $\langle(\sigma/r)^6\rangle$, $\langle(\sigma/r)^7\rangle$, and $\langle(\sigma/r)^{12}\rangle$ vs density.

FIG. 3. Energy per particle (in °K) vs volume (in cm^3/mole).

space adequately for a 500-particle system would have required a run of about 150 000 configurations—which would be both expensive and unwise considering the uncertainties in the intermolecular potential.

The additional runs at $\rho = 1.12$ were done for A and B values which, when scaled to the higher densities of $\rho = 1.23$ to 1.5, would be near the minimum in $\langle H \rangle$. Once this was done it was possible to see in which direction these parameters were moving,
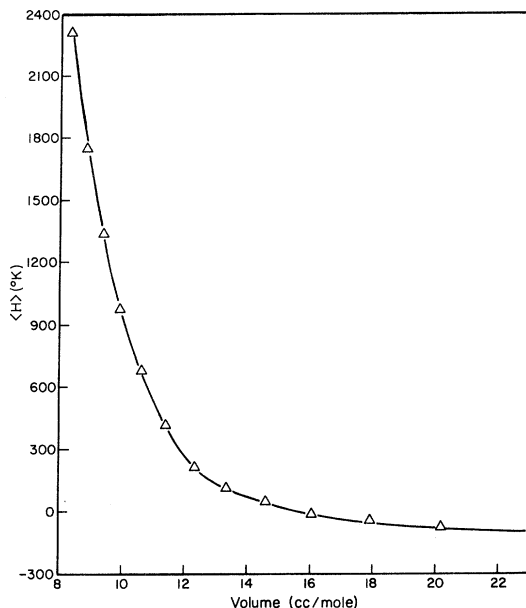
and do a few more runs in order to follow the minimum in $\langle H \rangle$ up to a density of $\rho = 1.87$ (and a pressure of 112 kbar).

In order to calculate the thermodynamic pressure, $P = \rho^2 \partial E / \partial \rho$, the energy-vs-density curve was fitted
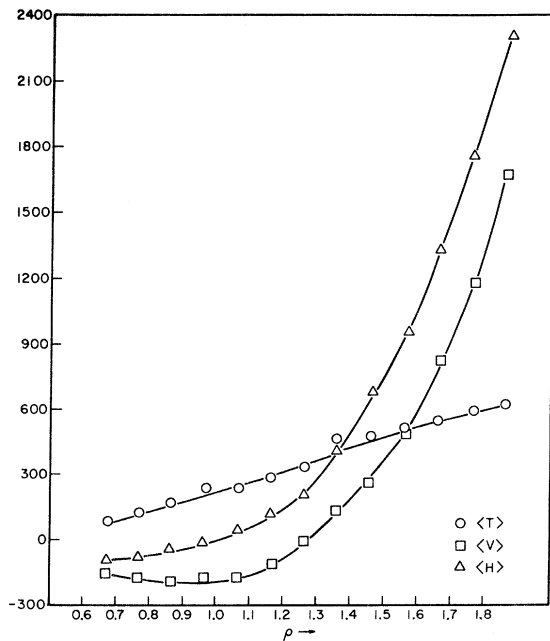

FIG. 2. Kinetic, potential, and total energy per molecule (in °K) vs density (in molecules/σ^3).
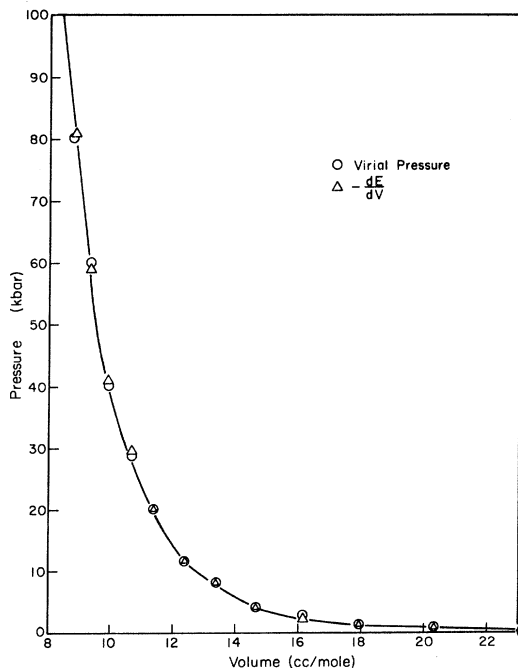

FIG. 4. Pressure vs volume (the equation of state).

TABLE III. A short summary of results. P_1 is the virial pressure calculated by (2.15) and P_2 is the thermodynamic pressure $\rho^2 dE/d\rho$.

ρ	T	V	H	P_1	P_2	Volume (cm^3/mole)
0.676	76.4427	−161.919	−85.4714	−2.0	1.4	23.08
0.77	103.058	−183.078	−80.02	331.4	315.7	20.26
0.87	152.239	−212.639	−60.40	1 042	1 061	17.93
0.97	154.842	−178.792	−23.95	2 702	2 449	16.08
1.07	226.353	−189.183	37.17	4 354	4 751	14.58
1.17	229.950	−100.240	129.71	8 425	8 265	13.33
1.27	277.140	− 11.340	265.80	13 559	13 319	12.28
1.37	333.273	112.067	445.34	20 578	20 300	11.39
1.47	457.195	220.195	677.39	28 302	29 708	10.61
1.57	477.701	481.109	958.81	41 934	42 252	9.94
1.67	497.776	821.614	1319.39	60 091	58 991	9.34
1.77	593.518	1170.73	1764.25	80 907	81 516	8.81
1.87	615.667	1685.163	2300.83	110 190	11 221	8.34

with a sixth-degree polynomial using a least-squares fitting process. The agreements between the energies were determined by the Monte Carlo integration combined with scaling and those calculated by the least-squares fit were good to within a few degrees kelvin (and especially good for the high-density region where the deviation was less than 0.5%). The agreement between the virial and thermodynamic pressures was also good.

IV. NUMERICAL RESULTS

The results of our calculations are summarized in the figures and tables below. In all, 130 points were obtained for the energy-vs-density curve, and thirteen of these are listed in the tables. As noted in Sec. III, the data (all 130 points) were fitted with

a sixth-degree polynomial in order to obtain the thermodynamic pressure $\rho^2 dE/d\rho$. This fit yielded the coefficients

$$a_0 = 4.005\,053 \times 10^2, \quad a_1 = -2.843\,095 \times 10^3,$$

$$a_2 = 7.397\,826 \times 10^3, \quad a_3 = -1.058\,733 \times 10^4,$$

$$a_4 = 8.200\,409 \times 10^3, \quad a_5 = -3.042\,918 \times 10^3,$$

$$a_6 = 4.651\,104 \times 10^2.$$

Table I gives a summary of the 256-particle calculations at $\rho = 0.694$, 0.9, and 1.12. These were used in scaling to obtain the results listed in Tables II and III for densities other than 0.694, 0.9, and 1.12, and from them, energies and virial pressures can be obtained for any density from $\rho = 0.67$ to $\rho = 1.87$. Table IV is a summary of the
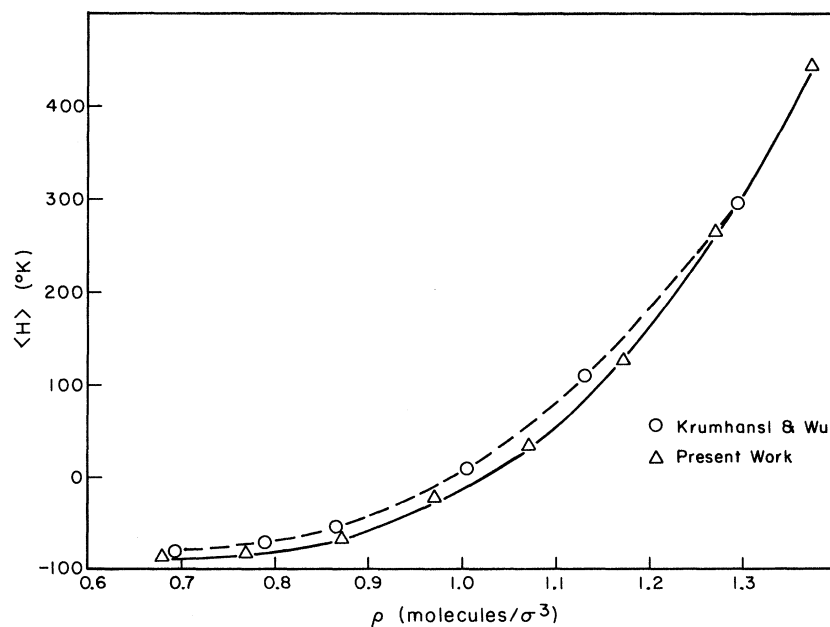

FIG. 5. Comparison of the energy-vs-density curves for the Lennard-Jones potential with the Krumhansl and Wu cluster results.

TABLE IV. Results of the Krumhansl and Wu cluster-expansion calculation for the Lennard-Jones potential.

ρ(molecules/σ^3)	V(cm^3/mole)	E(°K)	E^1(°K; by Monte Carlo)
0.694	22.47	−77.6	−77.54
0.778	20.0	−71.6	−68.43
0.864	18.0	−53.8	...
1.015	15.31	12.25	
1.137	13.7	107.1	
1.292	12.09	298	

TABLE V. Experimental data of Stewart.

ρ(molecules/σ^3)	V(cm^3/mole)	P(bar)
0.689	22.65	0
0.74	21.0	196.1
0.78	20.0	392.2
0.81	19.2	588.4
0.87	18.0	980.7
0.97	16.1	2 003
1.03	15.1	2 942
1.09	14.3	3 923
1.18	13.2	5 884
1.26	12.4	7 845
1.32	11.8	9 806
1.38	11.3	11 768
1.47	10.6	15 691
1.54	10.1	19 613

results of the Krumhansl and Wu cluster calculations with the Lennard-Jones potential. Using their wave function, we used the Monte Carlo integration program to check their calculations for $\rho = 0.694$ and $\rho = 0.778$ and found good agreement with their energies. Table V gives the results of compressibility experiments on solid hydrogen by Stewart.[11] Table VI lists the Krumhansl and Wu cluster results for two other potentials, the Buckingham exp-6 potential and the nonspherical Wang Chang potential, and Table VII gives a summary of our investigation of the Buckingham exp-6 potential. The results listed in the tables are displayed graphically in Figs. 1–7.

V. DISCUSSION OF RESULTS

A. Comparison of Theory and Experiment

We have obtained an equation of state for solid hydrogen which is in general agreement with the experimental data of Stewart[13] in the low-pressure range. Our curve agrees well with that obtained by Stewart for $V > 16$ cm^3/mole, but our results begin to diverge from the experimental data as the volume is decreased below 16 cm^3/mole. We have however been able to calculate a ground-state equilibrium energy which is in better agreement with experiment than that obtained by Krumhansl and Wu.[2] We obtained a ground-state energy of $- 85.47$ °K at a volume of 23.08 cm^3/mole as compared with the Stewart value of $- 93.47$ °K at $V = 22.65$ cm^3/mole. The Krumhansl and Wu cluster

calculations yielded energies of $- 77.6$ °K for the Lennard-Jones potential and $- 79.5$ °K for the Buckingham exp-6 potential at a volume of 22.47 cm^3/mole. Our calculations using the Lennard-Jones potential have led to an equation of state for solid hydrogen which is in better agreement with experiment than the results of the Krumhansl and Wu cluster calculations for the Lennard-Jones potential, but considerably worse than their results for the Buckingham exp-6 and Wang Chang potentials (see Figs. 5 and 6). We have however been able to extend the equation of state to very high pressures.

B. Summary and Conclusions

Our equation of state for solid hydrogen covers the pressure range 0–112 kbar. An estimate of the degree of uncertainty in the energy can be made by noting that if we do two Monte Carlo runs at the same values of the parameters A and B but starting from two different initial particle configurations, we will obtain energies which may vary by as much as 2–3°. We can safely say, however, that the over-all uncertainty in our equation of state for the Lennard-Jones potential is less than 2%. This

TABLE VI. The ground-state energy per molecule and the pressure for the Buckingham exp-6 and Wang Chang potential from the Krumhansl and Wu cluster calculations.

ρ(molecules/σ^3)	V(cm^3/mole)	exp-6 E(°K)	P(bar)	Wang Chang E(°K)	P(bar)
0.694	22.47	−79.5	0	−76.8	0
0.778	20.0	−73.9	397.1	−73.9	289.3
0.864	18.0	−57.2	1 010	−61.2	847.3
0.970	16.10	−18.9	2 393	−32.13	1 961
1.032	15.10	17.6	3 854	− 2.8	3 099
1.083	14.40	53.6	5 168	26.4	4 119
1.172	13.30	137	8 061	95.0	6 619
1.247	12.50	228	11 376	172	9 522
1.380	11.30	...	...	357	16 570
1.443	10.80	566	...	470	...
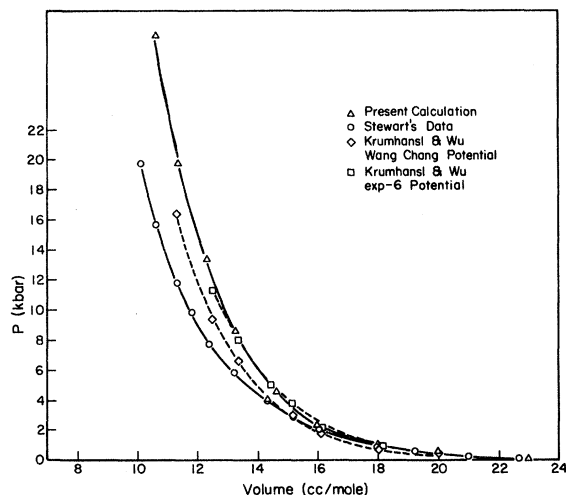
FIG. 6. Comparison of the equation of state with
earlier theoretical and experimental work.

TABLE VII. The ratio of kinetic-to-total energy for
$\rho = 1.37$ to $\rho = 3.27$.

ρ	$\langle T \rangle / \langle H \rangle$	$\sim P$(kbar)
1.37	0.75	21
1.47	0.68	28
1.57	0.50	42
1.67	0.38	60
1.77	0.34	81
1.87	0.27	110
1.97	0.22	147
2.07	0.18	193
2.17	0.15	249
2.27	0.122	318
2.37	0.119	396
2.47	0.101	493
2.57	0.088	608
2.67	0.076	744
2.77	0.066	903
2.87	0.058	1087
2.97	0.051	1300
3.07	0.045	1545
3.17	0.040	1824
3.27	0.036	2143

accuracy is adequate considering the uncertainty
in the potential.

At high pressures, the deviation from the ex-
perimental data is very large for the Lennard-Jones
potential (see Fig. 6). It is apparent that the re-
pulsive part of the potential for high densities is
much too strong and that we can only hope for a
qualitative understanding of the equation of state in
this area. One very striking feature of the energy
at high densities ($\rho > 1.5$) should, however, be
noted. By looking at Fig. 2 we can see that the
kinetic-energy expectation value $\langle T \rangle$ is growing in
a more or less linear way while the total energy
$\langle H \rangle$ is growing much more rapidly. By doing one
more run at $\rho = 1.12$ and scaling, we were able to
obtain approximate values of $\langle T \rangle$ and $\langle H \rangle$ for the

Lennard-Jones potential for densities up to 2.17
(and pressures ~ 2000 kbar). Figure 8 and Table
VIII show the ratio $\langle T \rangle / \langle H \rangle$ for the high-density re-
gion, and it is striking that for pressures greater
than 600 kbar this ratio is down to ~ 0.05–0.10;
i.e., the kinetic energy is contributing only 5–10% of
the total energy. This suggests that in the 1–2-Mbar
range where the suspected transition from the
molecular to metallic phase is thought to occur,
classical calculations of the equation of state may
become possible. In these calculations, the kinetic-
energy contribution to the total energy is calculated
from zero-point motion in the lattice and is usually
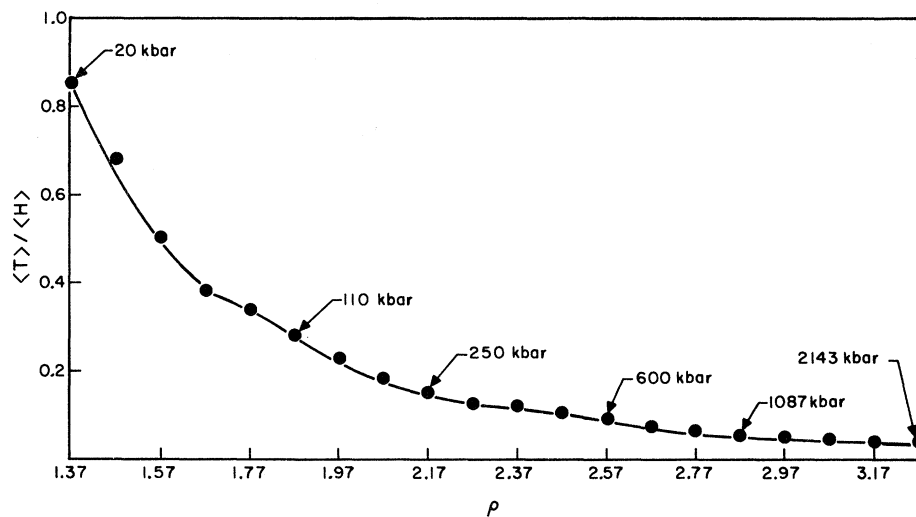quite small (~ 5–15%).

FIG. 7. Ratio of $\langle T \rangle /$
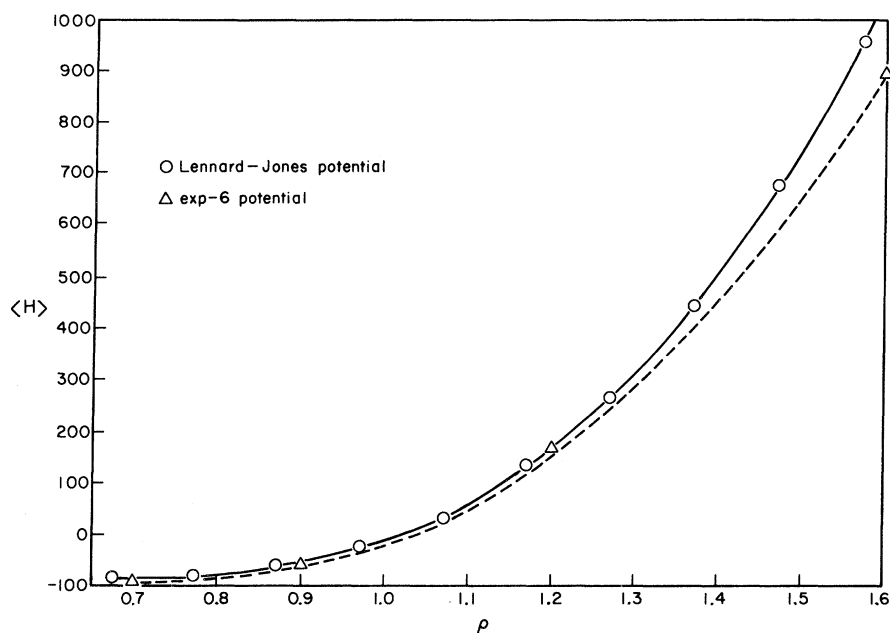$\langle H \rangle$ for the Lennard-Jones
potential for $\rho = 1.4$–3.2.

FIG. 8. Comparison of the energy-vs-density curves for the Lennard-Jones and exp-6 potentials for $\rho = 0.7-1.6$.

The possibility of doing accurate "classical" calculations for solid hydrogen at high densities is very important since it would both reduce the cost of determining the equation of state in this region by an order of magnitude, and also open the possibility of investigating many other intermolecular potentials. Therefore, we have examined this question in detail in an accompanying paper. It must however be noted that the data used in Fig. 7 were obtained by using the Lennard-Jones potential, which we have already noted is not accurate in this region, giving energies which are too large. The contribution of the kinetic energy in this region could thus be as high as 15-20%, and further investigations using Monte Carlo and other potentials will be necessary to verify this conjecture.

C. Brief Investigation of Buckingham exp-6 Potential

We have noted that the Lennard-Jones potential is not a very good approximation for hydrogen for high densities. The earlier cluster work by Krumhansl and Wu has shown that better agreement between theory and experiment can be obtained by using the modified Buckingham exp-6 potential, and it was decided that a brief investigation of this potential using Monte Carlo could be useful. We have determined the ground-state energy for the exp-6 potential at four values of the density and found good agreement with the Lennard-Jones results up to a density of $\rho \sim 1.3$. Above $\rho \sim 1.3$ the energy for the exp-6 potential is considerably lower than the energy for the Lennard-Jones potential, and in good agreement with the results of Krumhansl and Wu for this potential. The results

TABLE VIII. Results of the investigation of the Buckingham exp-6 potential.

108-particle searches			
	A	B	$\langle H \rangle$
$\rho = 0.9$	25	1.10	-59.4
		1.15	-60.4
	30	1.05	-51.7
		1.10	-63.6
		1.15	-62.9
		1.20	-56.1
	35	1.15	-59.5
$\rho = 1.2$	33	1.15	154.3
	35	1.10	160.2
		1.15	141.8
		1.20	146.9
	37	1.15	142.1
$\rho = 1.6$	40	1.15	954
	45	1.10	950
		1.15	929
		1.20	933
		1.25	958
	50	1.15	923
	55	1.15	921
		1.20	929
	60	1.10	945
		1.15	919
	65	1.15	930
Final results ($\langle T \rangle / \langle H \rangle = 0.43$)			
ρ	A	B	$\langle H \rangle$
0.694	15	1.15	-88.28
0.9	30	1.10	-54.68
1.2	35	1.15	164.74
1.6	60	1.15	896.4

of this investigation are listed in Table VII.

For $\rho = 0.694$ we did only one 108-particle run, assuming that the minimum in $\langle H \rangle$ for the exp-6 potential would lie very close to the minimum for the Lennard-Jones potential. For this value of the density, the contribution of the repulsive part of the potential is small so this should be a good assumption. For $\rho = 0.9$ and 1.2, a parameter search was performed using the 108-particle system and then one 256-particle run was done using the values for A and B which determined the minimum in the 108-particle search. The agreement between the energies obtained by using the 108- and 256-particle systems with the same A and B values was $\sim 9°$ at $\rho = 0.9$ and $\sim 23°$ at $\rho = 1.2$. It was thus apparent that the 256-particle system would not be large enough to give us an accurate energy at the next density which we wanted to look at, $\rho = 1.6$. For $\rho = 1.6$ we again made a parameter search with the 108-particle system and attempted to refine the energy by this time using a 500-particle system. A final run of 80 000 configurations of which the first 20 000 were discarded was done; even so the en-

ergy had not yet settled down very well. The energy we have listed for $\rho = 1.6$ is good only to about 20° whereas all of our other energies are good to within 1–2°. We can see however that there is a considerable difference between the energies yielded by the exp-6 and Lennard-Jones potentials for densities greater than 1.3, and that the exp-6 potential yields a much better agreement with experiment.

One last point of importance should be noted. For $\rho = 1.6$ the ratio of $\langle T \rangle / \langle H \rangle$ is slightly less for the exp-6 potential than for the Lennard-Jones, thus confirming our conjecture that at high densities the "classical harmonic" approximation may be valid.

ACKNOWLEDGMENTS

*Work supported by the U. S. Atomic Energy Commission under contract No. AT(30-1)-3699, Technical Report No. NYO-3699-52, and the National Science Foundation under grant No. GP-27355.

[1] E. Wigner and H. B. Huntington, J. Chem. Phys. 3, 764 (1965); R. Kronig, J. deBoer, and J. Korringa, Physica 12, 245 (1946); W. C. DeMarcus, Astron. J. 63, 2 (1958); A. A. Abrikosov, Astron. Zh. 31, 112 (1954).

[2] N. W. Ashcroft, Phys. Rev. Letters 21, 1748 (1968).

[3] J. A. Krumhansl and S. Y. Wu, preceding paper, Phys. Rev. B 5, 4155 (1972); Phys. Letters 28A, 263 (1968).

[4] J. P. Hansen and D. Levesque, Phys. Rev. 165, 293 (1968).

[5] J. P. Hansen, Phys. Rev. 172, 919 (1968).

[6] A. M. Michels, W. deGraaf, and C. A. ten Seldam, Physica 26, 393 (1960).

[7] I. B. Srivastava and A. K. Barua, Indian J. Phys. 35, 722 (1965).

[8] W. I. McMillan, Phys. Rev. 138, A442 (1964).

[9] W. Kolos and C. C. J. Roothaan, Rev. Mod. Phys. 32, 219 (1960).

[10] N. Metropolis et al., J. Chem. Phys. 21, 1087 (1953).

[11] W. W. Wood and F. R. Parker, J. Chem. Phys. 27, 720 (1957).

[12] D. Schiff and L. Verlet, Phys. Rev. 160, 208 (1967).

[13] J. W. Stewart, J. Chem. Phys. Solids 1, 146 (1956).